

# Synthesis of Tungsten Oxide (WO<sub>3</sub>) Nanoparticles with EDTA by Microwave Irradiation Method

V. Hariharan\*<sup>1</sup>, V. Aroulmoji<sup>2</sup>, C. Sekar<sup>3</sup>, A. Shanthakumar<sup>1</sup>, M. Kumara Dhas<sup>1</sup>, Edinbero Komagan, K. Kalamegam<sup>1</sup>

<sup>1</sup> Department of Physics, Mahendra Arts and Science College (Autonomous), Kalippati, Namakkal, Tamilnadu, India

<sup>2</sup> Centre for Research and Development, Mahendra Educational Institutions, Mallasamudiram, 637503, Tamilnadu, India

<sup>3</sup> Department of Bioelectronics and Biosensors, Alagappa University, karaikudi, Tamilnadu, India

**ABSTRACT:** This paper presents synthesis and characterization of tungsten oxide (WO<sub>3</sub>) nanoparticles using EDTA as surfactant by simple household microwave irradiation (2.45 GHz) method. The samples were characterized using powder X-ray diffraction (XRD), transmission electron microscopy (TEM) and UV-visible diffusion reflectance spectroscopy (UV-VIS-DRS). Powder XRD results revealed that both samples prepared with and without surfactant crystallize in the orthorhombic structure corresponding to WO<sub>3</sub>·H<sub>2</sub>O phase. Subsequent annealing under identical conditions (600°C/air/6 h) led to significantly different products i.e. monoclinic W<sub>17</sub>O<sub>47</sub> from surfactant free sample and similarly monoclinic phase of WO<sub>2.72</sub> from EDTA assisted sample. Blue emission was observed through UV-VIS-DRS with band gap energy around 3.28 and 3.47 eV for EDTA assisted samples respectively.

**KEYWORDS:** EDTA, Polymer, Surfactant, WO<sub>3</sub>, Oxygen deficient, TEM

© 2015 mahendrapublications.com, All rights reserved

## 1. INTRODUCTION

Nanotechnology was regarded as a science fiction in the field of science and technology until the recent past, something impossible and unattainable. But over time, nanotechnology and its uses among different facets of the society such as agriculture, households gadgets and industry. Whereas, nanotechnology is widely accepted and practiced in the field of environmental protection [1]. It is well known that Nanotechnology is the engineering of functional systems at the molecular scale or through tiny engineering. In essence, nanotechnology is the probability to build things from the bottom up using scientific techniques and tools that are currently developed today to come up with advanced, complete, and highly usable and essential products. The term "nanotechnology" has evolved over the years via terminology drift to mean micro technology, such as nano powders, and other things that are nanoscale in size, but not that have been purposefully built from nanoscale components. Recently, the alternate term to represent the original meaning of nanotechnology is zettatechnology [2]. Two basic structures have to be distinguished in nanotechnology. Pointed-shaped structures known as fullerenes and stretched structures like carbon nanotubes are the two basic structures. The best explored fullerene is the C<sub>60</sub> fullerene. It is called Bucky ball after the famous architect Richard Buckminster Fuller who constructed a lot of geodesic domes. These are buildings which possess the structure of the C<sub>60</sub> fullerene [3]. One-dimensional (1D) self-assembled single-crystalline hexagonal tungsten oxide (h-WO<sub>3</sub>) nanostructures were synthesized by hydrothermal method at 180°C using sodium tungstate, ethylene diamine tetra acetic (EDTA) salts of

sodium or ammonium, and sodium sulfate by Jang-Hoon Ha et al [4]. The synthesis of 1D self-assembled h-WO<sub>3</sub> nanowires, bundles and urchin-like structures was differentiated by means of Na<sup>+</sup>- and NH<sub>4</sub><sup>+</sup>- based EDTA salt solutions. Deepa et al [5] pointed out that by electrochemically controlling the structure of the surface aggregates; the grain microstructure has been optimized to yield mesoporous thin films of tungsten oxide (WO<sub>3</sub>) at the electrode-electrolyte interface in a peroxo tungstate sol in the presence of a structure-directing agent (Triton) at room temperature.

Taylor et al [6] synthesized half-micron-thick tungsten oxide films by the sol-gel method onto indium tin oxide (ITO) coated soda lime silicate substrates. The samples were fired with carbon dioxide laser which increased the electrochromic response with increased firing temperature up to the point where crystallization of the tungsten oxide retarded electrochromic response. Thus they concluded that electrochromic windows with good properties were made by laser firing sol-gel-derived tungsten oxide films.

The fabrication and characterization of tungsten oxide nanofibers using the electrospinning technique and sol-gel chemistry was successfully demonstrated by Guan Wang et al [7]. They insisted the potential applications of the electrospun tungsten oxide nanofibers as a sensor material for gas detection. Ultrafine tungsten and tungsten oxide powders with controllable particle size and structure had been synthesized by a reverse microemulsion-mediated synthesis method by Liufeng Xiong et al [8]. The interesting applications in various fields such as catalysis, electronics,

\*Corresponding Author: vhariharan06@gmail.com

Received: 18.10.2016

Accepted: 20.11.2016

Published on: 30.11.2016

illumination and gas sensors were illustrated.

A simple and inexpensive method to produce thin films of nano structured tungsten oxide was described by Erika Widenkvist et al [9]. They reported that the potential of this inexpensive synthesis method to produce large-area coatings of nanostructured tungsten oxide as well as patterned films makes it interesting for several different applications such as batteries, gas sensors, and photocatalysts. Electrochromic tungsten oxide film was fabricated by a new soft chemistry route, for electrochromic systems by Jin-Ho Choy et al [10]. They found that depending on the concentration of PAA coating solution (1.0-3.0 wt%), the thickness and tungsten oxide content of the film were found to vary, therefore, the electrode property of the PAA/WO<sub>3</sub> layer could easily be controlled.

Mesoporous semiconducting films consisting of preferentially orientated monoclinic-phase nanocrystals of tungsten trioxide had been prepared using a novel version of the sol-gel method by Clara Santato et al [11]. They illustrated that the shape and size of WO<sub>3</sub> nanoparticles, the porosity, and the properties of the films depend critically on preparation parameters, such as the tungstic acid/PEG ratio, the PEG chain length, and the annealing conditions. Well-crystallized WO<sub>3</sub> films combine excellent photo response to the blue region of the solar spectrum, up to 500 nm, with good transparency at wavelengths larger than 550 nm. They suggested that the particular applications of these nanocrystalline WO<sub>3</sub> films include photoelectrochemical and electrochromic devices.

Jinmin Wang et al [12] reported the synthesis of uniform crystalline WO<sub>3</sub> nanorods and their assembly without any surfactants. WO<sub>3</sub> nanorods had been synthesized by using a facile hydrothermal process without employing lithium ions and sulfates. The resulting WO<sub>3</sub> nanorod film exhibits high electrochromic stability and comparable color display, contrast, and coloration/bleaching response was reported.

Photo luminescent behaviour of BaWO<sub>4</sub> powders processed in microwave-hydrothermal was observed by Cavalcante et al [13]. Photoluminescence (PL) at room temperature was observed in BaWO<sub>4</sub> powders processed in microwave hydrothermal at 140°C in different times. PL behaviour was attributed to the existence of distortions on the [WO<sub>4</sub>] tetrahedron groups caused by microwave radiation. XRD studies of thermally stable mesoporous tungsten oxide synthesized by a template sol-gel process from tungstic acid precursor had been done by WeiWang et al [14]. This work opens a new pathway for the preparation of mesoporous tungsten oxide films using tungstic acid precursor with many advantages including reduced cost, easy handling, and insensitivity to moisture.

Abraham Wolcott et al [15] reported the synthesis of ultrathin WO<sub>3</sub> nanodisks using a wet chemical route with polyethylene glycol (PEG) as a surface modulator. The reported nanodisk structure was based on the interaction of the non ionic 10000 g/mol PEG molecules with tungsten oxoanion precursors. The large flat surface area and high aspect ratio of the WO<sub>3</sub> nanodisks were potentially useful in

PEC cells. It was reported that using PEG-10000 as a surface modulator that adsorbs preferentially to the (010) crystal face and thereby inhibits crystal growth and the nanodisk formation is critically influenced by the interaction between PEG and the WO<sub>3</sub>.2H<sub>2</sub>O precursors as compared to other studies resulting in spherical nanoparticles.

Fusong Jiang [16] prepared tungsten oxide and iridium oxide porous films and their electro chromic properties were analysed. Sol-gel preparation of porous tungsten oxide and iridium oxide films by using polystyrene template was described. Cyclic voltammograms showed that the electro chromic properties of the porous films were 1-2 orders better than those of relative non-porous films. The porous films are expected to be used to build-up a new ECD with better electro chromic properties than normal ECD Composed by corresponding non-porous films.

Deepa et al [17] studied the influence of polyethylene glycol template on microstructure and electro chromic properties of tungsten oxide. Electro chemical synthesis of tungsten oxide (WO<sub>3</sub>) thin film nano structures by potentiostatically controlling the surface aggregates formed at the electrode-electrolyte interface, in the presence of a polymeric template (polyethyleneglycol400) from a plating sol of peroxo tungstic acid (PTA) is presented. This film also exhibits fast switching between the clear and blue states. These are repercussions of the mesopore structure and the interconnected nanocrystallite phase.

A comparison of electrochromic properties of sol-gel derived amorphous and nano crystalline tungsten oxide films was reported by Deepa et al [18]. A pristine acetylated peroxotungstate sol with and without 4wt% of oxalic acid dehydrate (OAD) yielded nanocrystalline and amorphous tungsten oxide (WO<sub>3</sub>) films respectively by dip coating technique. Band gap widening upon lithium insertion observed for both films, is a repercussion of Burstein-Moss effect and structural changes that occur upon coloration was also reported.

Sol-gel derived tungsten oxide films with pseudocubic triclinic nanorods and nanoparticles were synthesized by Srivastava et al [20]. Tungsten oxide films were deposited using acetylated peroxotungstic acid as the precursor material adopting sol-gel dip coating route, followed by thermal treatment. The kinetic mechanisms responsible for the formation of nanorods have also been elucidated. It was reported that both the nanorods and the particles exhibited a pseudocubic triclinic crystal structure. Jiun-ChanYang et al [21] adopted solution-based synthesis of efficient WO<sub>3</sub> sensing electrodes for high temperature potentiometric NO<sub>x</sub> sensors. Electrode nanostructures as well as species at electrode-electrolyte interfaces have substantial influence on the sensitivity, response and recovery times of electrochemical sensors. YSZ-based potentiometric NO<sub>x</sub> sensors with WO<sub>3</sub> sensing electrodes have shown considerable promise for enhanced sensitivity had been reported.

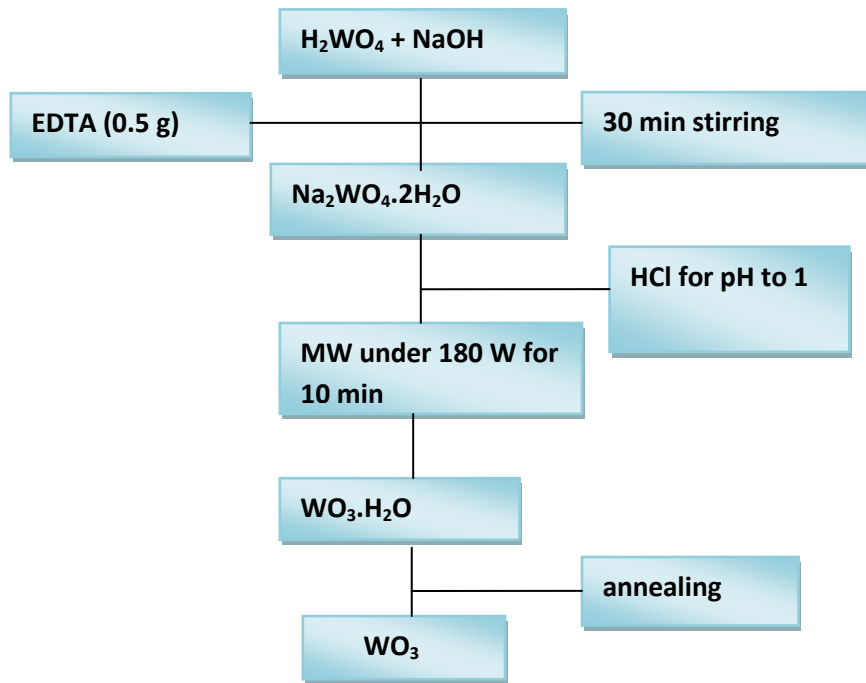


Fig 1. Synthesis of  $WO_3$  nanoparticles

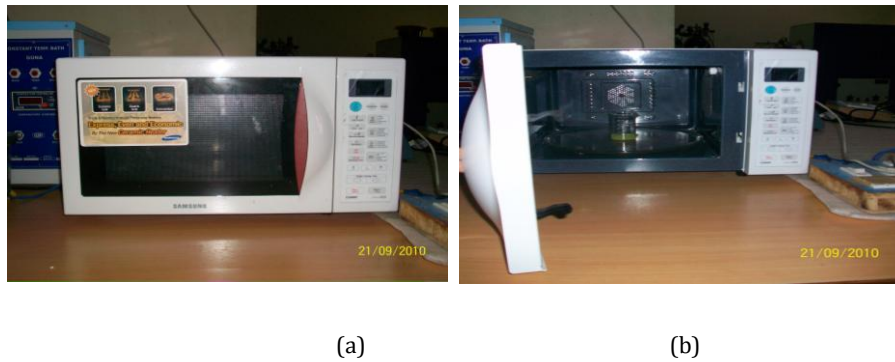


Fig. 2. Microwave Oven used for synthesis (a) Outer view (b) Inner view



Fig.3. Horizontal Tubular Furnace used for annealing the samples

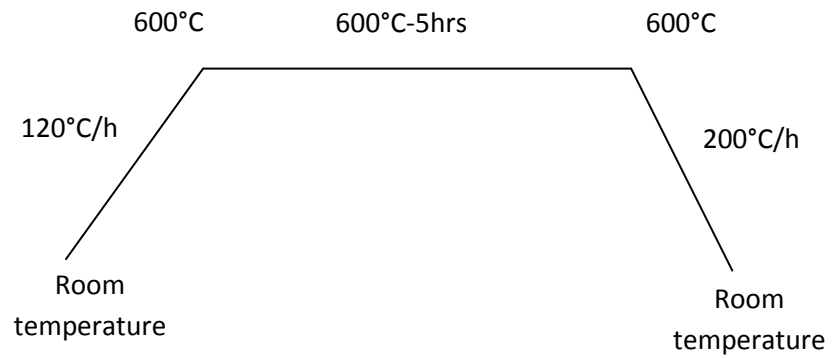


Fig. 3. Temperature Profile of as prepared sample ( $WO_3.H_2O$ )

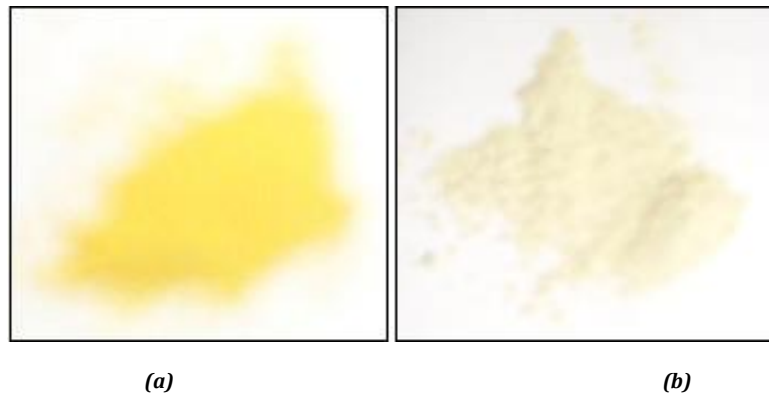


Fig.5. Synthesized samples (a)  $WO_3.H_2O$  (b)  $WO_{2.72}$

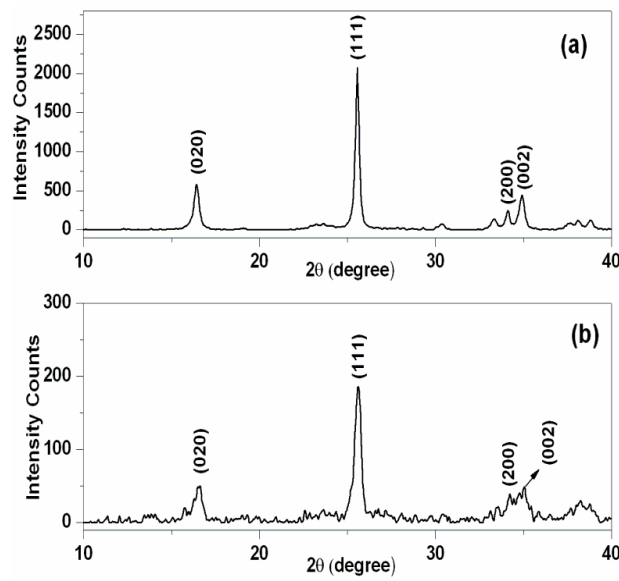


Fig.6.  $WO_3.H_2O$  (a) without EDTA (b) with EDTA

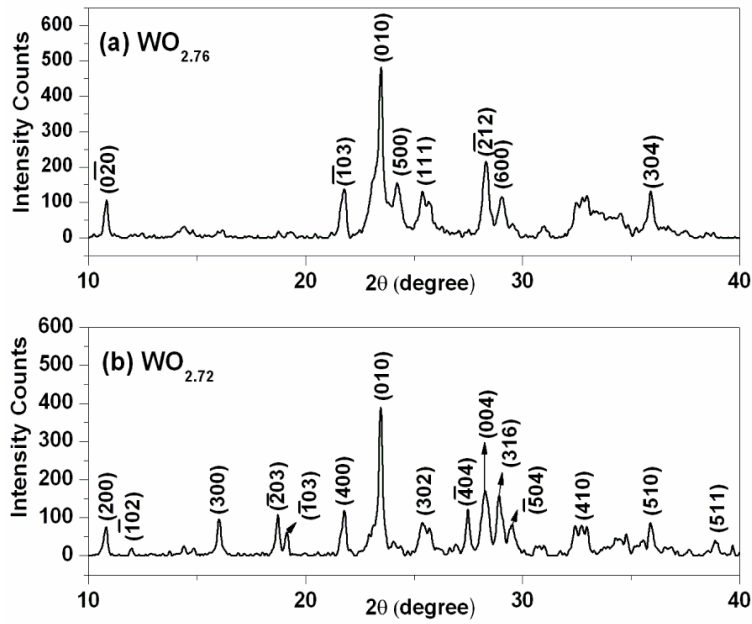


Fig.7. (a)  $WO_{2.76}$  (without EDTA) & (b)  $WO_{2.72}$  (with EDTA)

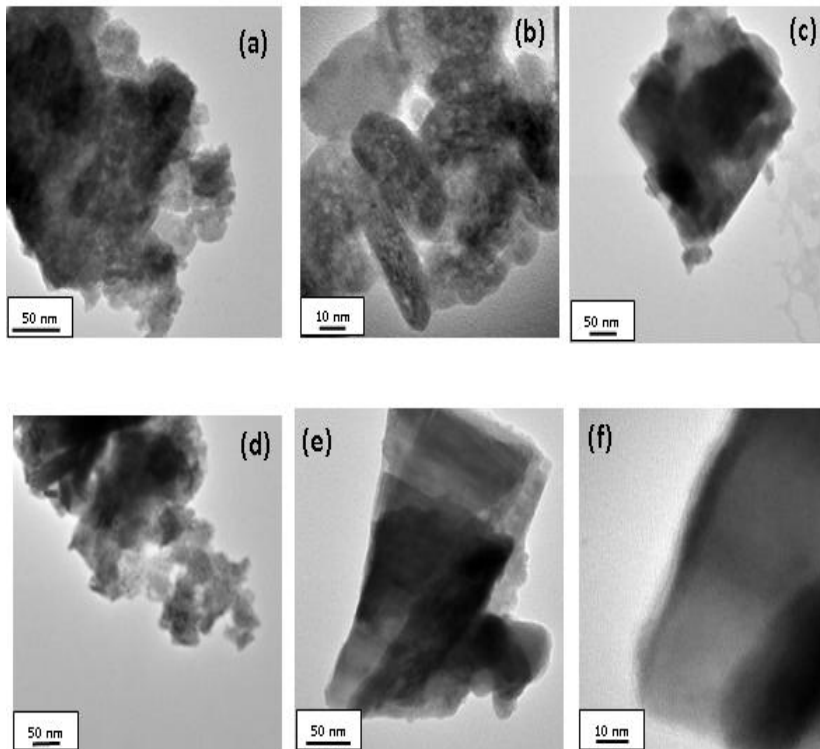


Fig.8. (a-b)  $WO_3 \cdot H_2O$  without EDTA (c)  $WO_{2.76}$  (d)  $WO_3 \cdot H_2O$  with EDTA (e-f)  $WO_{2.72}$

Influence of annealing on electrochromic performance of template assisted, electrochemically grown, nanostructured assembly of tungsten oxide was studied by Deepa et al [22]. Nano structured tungsten oxide ( $\text{WO}_3$ ) thin films have been electrochemically grown from a self-assembly of sodium dodecyl sulfate-tungsten oxide aggregates at the electrode-electrolyte interface. Poor color-bleach rates observed for the films annealed at 250 and 500°C are attributed to pore shrinkage, high density and crystallinity.

Deepa [23] et al compared spin coated versus dip coated electrochromic tungsten oxide films. Structure, morphology, optical and electrochemical properties. A sol-gel derived acetylated peroxy tungstic acid sol encompassing 4wt.% of oxalic acid dihydrate (OAD) has been employed for the deposition of tungsten oxide ( $\text{WO}_3$ ) films by spin coating and dip coating techniques, in view of smart window applications. A comparative study of spin and dip coated nanostructured thin films (annealed at 250 °C) revealed a superior performance for the cycled dip coated film in terms of higher transmission modulation and coloration efficiency in solar and photopic regions, faster switching speed, higher electrochemical activity as well as charge or age capacity. While the dip coated film could endure 2500 color bleach cycles, the spin coated film could sustain only a 1000 cycles. The better cycling stability of the dip coated film which is a repercussion of a balance between optimal water content, Porosity and grain size hints at its potential for electrochromic window applications.

In the present work, it is proposed to synthesize  $\text{WO}_{2.72}$  nanoplate like morphology by simple microwave irradiation method using EDTA as surfactant. The role of EDTA in the synthesis of  $\text{WO}_{2.72}$  nanoparticles will be investigated in detail. The  $\text{WO}_{2.72}$  will be characterized using powder XRD, TG-DTA, FT-IR, TEM and UV-VIS DRS techniques in order to assess the quality of the products and to find the suitability for specific applications.

## 2. EXPERIMENTAL PROCEDURE

The usually prepared solution was prepared by dissolving 2.49g of tungstic acid ( $\text{H}_2\text{WO}_4$ ) in 10 ml of sodium hydroxide (NaOH) with one molar ration concentration. It results in yellow colored hydrated sodium tungstate solution due to proton exchange protocol process. Subsequently 0.5g (~20% of tungstic acid) of EDTA was added and several drops of HCl were introduced to attain the pH value of 1. Here the added HCl can act as a precipitating agent and also medium for the product to have desired morphology. In order to respond microwave quickly double distilled water (~50% of the total volume) was added, simultaneously the final solution was transformed into microwave oven under power of 180W for 10min (choice was random manner). The surrounding water present in the product was removed by drying process at 60°C in air for 1 hr. The process was repeated in the absence of EDTA salt under the identical conditions. Both products resulted yellow colored powder that was annealed at 600°C in air for 6 hrs to attain crystalline anhydrous tungsten oxide.

The horizontal tubular furnace with two zones and temperature controllers is shown in Fig. 2. The maximum

temperature of the furnace is 1400°C and the operating temperature is around 1300°C. The thermal analysis was performed on SDT Q600 V8.3 Build 101. The X-ray powder diffraction (XRD) patterns of all the samples were measured on a Bruker AXS D8 advanced diffractometer with monochromatic  $\text{CuK}\alpha$  - radiation ( $\lambda = 1.5406\text{\AA}$ ). The TEM images and a Selected-area electron diffraction (SAED) were recorded on a Technai G20-stwin High resolution electron microscope (HRTEM) using an accelerating voltage of 200 kV. The optical properties were analyzed by UV-VIS diffusion reflectance spectroscopy using CARY 5E UV-VIS-NIR spectrophotometer (200 – 800 nm).

## 2.1 MICROWAVE IRRADIATION MECHANISM

Intercalation chemistry and interfacial polarization phenomenon play a major role in the synthesis of oxide based metal nanoparticles. Interfacial polarization is an effect which is very difficult to treat in a simple manner, and is most easily viewed as a combination of the conduction and dipolar polarization effects. In intercalation process the strong absorbing nature of tungstic acid and water at 2.45GHz which is responsible for the heating and to drive the reaction.



According to reaction (1), high concentrations of hydrated sodium tungstate would shift the reaction to the right ensuring the formation of  $\text{WO}_3$ , although many intermediate steps and thus compounds and phases may exist. It is thus the formation of  $\text{WO}_3$  should have dependence on the acid medium. To convert  $\text{WO}_4^-$  to neutral  $\text{WO}_3$ , excess divalent oxygen must be removed by microwave irradiation method. The thermal analysis was performed on SDT Q600 V8.3 Build 101. The X-ray powder diffraction (XRD) patterns of all the samples were measured on a Bruker AXS D8 advanced diffractometer with monochromatic  $\text{CuK}\alpha$  - radiation ( $\lambda = 1.5406\text{\AA}$ ). The TEM images and a Selected-area electron diffraction (SAED) were recorded on a Technai G20-stwin High resolution electron microscope (HRTEM) using an accelerating voltage of 200 kV. The optical properties were analyzed by UV-VIS diffusion reflectance spectroscopy using CARY 5E UV-VIS-NIR spectrophotometer (200 – 800 nm).

## 3. X-RAY DIFFRACTION ANALYSIS

Powder XRD results confirmed the phase formation (Fig.6) and the peaks could be indexed for orthorhombic phase (JCPDS card-43-0679). The crystallinity of  $\text{WO}_3 \cdot \text{H}_2\text{O}$  prepared without EDTA revealed sharp and stronger peaks to that of the sample using the surfactant EDTA. The annealed samples at 600°C in air for 6hrs resulted in oxygen deficient  $\text{WO}_{3-\delta}$  phase.

Fig. 7 shows the XRD pattern of annealed samples which could be assigned to the  $\text{W}_17\text{O}_{47}$  (JCPDS card-79-0171) and  $\text{W}_{18}\text{O}_{49}$  (JCPDS card-84-1516) phases with monoclinic structure. The oxygen content of EDTA assisted sample was found to be slightly lower than the surfactant free sample. XRD pattern of EDTA assisted  $\text{WO}_{2.72}$  contains more number of peaks and they are sharper when compared to the sample

prepared without surfactant. The EDTA enhances the crystallinity and reduces the oxygen content of the end product. In general, tungsten oxides easily lose oxygen and are represented as  $WO_{3-\delta}$ . The oxidation state of tungsten in  $WO_{2.72}$  lies between +4 ( $WO_2$ ) and +6 ( $WO_3$ ). With larger non-stoichiometry the defects preferentially accumulate at so called crystallographic shear planes along  $(l, m, 0)$  with the formation of edge-shared  $WO_6$  octahedra [23]. The intensity at (010) reflection in both the samples is greater than other peaks, suggesting that the formation of crystalline  $WO_{2.76}$  and  $WO_{2.72}$  nanosheets were oriented along the (010) direction.

EDTA has been widely used as chelating agent and as surface modulator in the synthesis of many nanostructured materials. The presence of sodium ion ( $Na^+$ ) in EDTA plays a crucial role in modifying the morphology of the product by adsorbing oxygen quickly during the annealing process. Thus, it appears that  $Na^+$  based EDTA salt has resulted self assembled tungsten oxide nanostructures [24]. The annealing of  $WO_3 \cdot H_2O$  prepared using EDTA resulted in oxygen deficient  $WO_{2.72}$ . This may be due to the formation of

intermediate sodium oxide ( $Na_2O$ ) during annealing process. The EDTA may also act as a driving force in producing such sheet like structure of  $WO_{2.72}$  during annealing process which is in agreement with the TEM analysis.

### 3.1 TEM STUDIES

Figs. 8a & 8b show the TEM micrographs of  $WO_3 \cdot H_2O$  synthesized without adding EDTA. Higher magnification picture reveals that the sample consisted of nanosized tablets of different dimensions. Upon annealing at  $600^\circ C$  in air for 6 hrs these tiny particles aggregated and resulted in platelet like morphology (Fig.8c). Fig. 8d shows the TEM image of  $WO_3 \cdot H_2O$  prepared using EDTA as surfactant. These micrographs showed that the nanosized crystals fairly well dispersed when compared to the sample grown without EDTA. Annealing effects on this sample under identical conditions led to platelets which are made up of a number of nanosheets with dimensions of the order of about 250 nm in length and 150 nm in breadth (Fig.8e) respectively. HR-TEM image of  $WO_{2.72}$  (Fig. 8f) reveals the 'd' spacing of the lattice fringes to be around 0.5 nm which corresponds to (102) plan in XRD pattern.

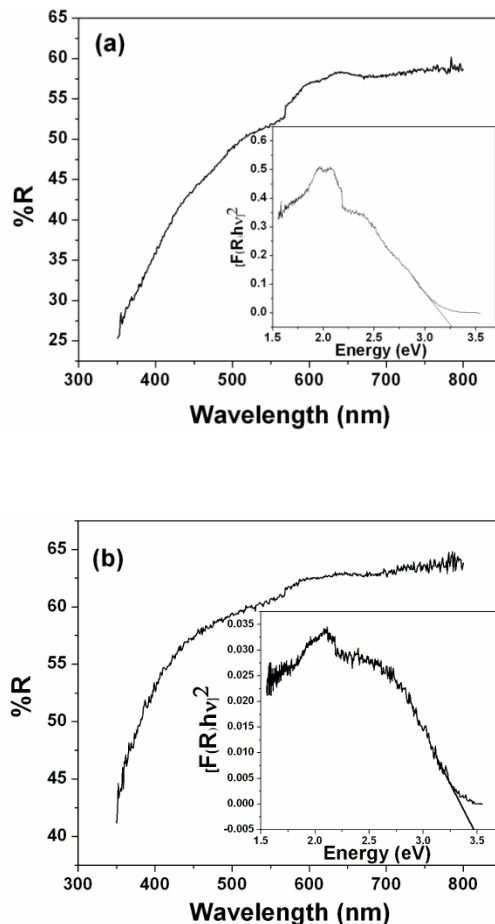


Figure 9. UV- VIS Diffusion Reflectance Spectroscopy of (a)  $WO_3 \cdot H_2O$  (b)  $WO_{2.72}$

### 3.2 UV- VIS DIFFUSION REFLECTANCE SPECTROSCOPY

Fig. 9 & 10 show the diffusion reflectance spectra of as prepared ( $\text{WO}_3 \cdot \text{H}_2\text{O}$ ) and annealed sample ( $\text{WO}_{2.72}$ ) respectively. The absorption from 550nm to 450nm towards lower wavelengths in the entire spectrum (blue shift) corresponds to the absorption edge of the solids. The band gap energy ( $E_g$ ) [24] for both the samples is extracted from UV-VIS DRS spectra as discussed below. The fundamental indirect allowed transitions of  $\text{WO}_{3-x}$  due to transition from O 2p electrons from the valence band to the W 5d conduction band.

The band gap energies ( $E_g$ ) have been calculated using Kubelka – Munk (K-M) model as described below. The K-M model at any wavelength is given by

$$\frac{K}{S} = \frac{(1 - R_\infty)^2}{2R_\infty} \equiv F(R_\infty)$$

$F(R_\infty)$  is the so called remission or Kubelka – Munk function, where  $R_\infty = R_{\text{sample}} / R_{\text{standard}}$

A graph is plotted between  $[F(R_\infty)h\nu]^2$  Vs  $h\nu$  and the intercept value gives the band gap energy  $E_g$  [25] of the individual sample (See insert of Fig. 11 ). Thus, the band gap energies were estimated as 3.28 and 3.47 eV for already prepared and annealed sample respectively. These band gap values reveals that the EDTA assisted samples having more optical conductivity than the surfactant free samples.

### 4. CONCLUSION

The successful synthesis of  $\text{W}_{18}\text{O}_{47}$  and  $\text{W}_{18}\text{O}_{49}$  nano particles by microwave irradiation method with and without using EDTA was carried out using EDTA as surface modulator. The powder XRD investigation confirms the prepared sample in both cases to be orthorhombic phase ( $\text{WO}_3 \cdot \text{H}_2\text{O}$ ) and the annealed samples ( $\text{WO}_{2.76}$  and  $\text{WO}_{2.72}$ ) were indexed as monoclinic structures compared to PEG, EDTA as surfactant yields oxygen deficient ( $\text{WO}_{2.72}$ ) samples. TEM observation clearly shows the role of EDTA in determining the size and shape with the dimensions of 250 nm in length and 150 nm in width. The UV-VIS DRS analysis indicates the band gap energies of the EDTA assisted samples to be lower than that of surfactant free samples. These results suggest that the surfactant EDTA enables the prepared plate like tungsten with reduced oxygen content. Nanoparticles with plate like morphology and sizes are required for unique applications in nanotechnology such as photon acceptors and super capacitors.

### REFERENCES

[1] Charles P. Poole, Frank J. Owens., 2003. *Introduction to nanotechnology*, 1-20.  
 [2] Ygao, Yband, Introduction to nanotechnology, 2003. *Nature* 71-110.  
 [3] *Nano system; Molecular Machinery, 200., manufacturing and computation*, 0-471.  
 [4] Jang-Hoon Ha, Muralidharan P, Kim D, 2009. hydrothermal synthesis and characterization of self

assembled h- $\text{WO}_3$ , Department of Materials Science and Engineering 373-1.

- [5] Deepa M, Kar M, Singh D. P, Srivastava A. K, Ahmad S, 2008. Influence of polyethylene glycol template on microstructure and Electrochromic properties of tungsten oxide, *Solar Energy Materials & Solar Cells* 92 170-178.  
 [6] Taylor D, J, Cronin J. P, Allard L. F, Birnie D. P., 1996. Microstructure of Laser-Fired, Sol-Gel-Derived Tungsten Oxide Films, *Chem. Mater.* 8 (7) 1396-1401.  
 [7] Wang G, Huang J. Y, Yang X, Gouma P. I, Dudley M., 2006. Fabrication and Characterization of Polycrystalline  $\text{WO}_3$  Nanofibers and Their Application for Ammonia Sensing, *J. Phys. Chem. B* 110 23777-23782.  
 [8] Liufeng Xiong, Ting He, 2006. Synthesis and Characterization of Ultrafine Tungsten and Tungsten Oxide Nanoparticles by a Reverse Microemulsion-Mediated Method, *Chem. Mater.* 18 2211-2218.  
 [9] Christopher S, Blackman, Parkin P. I, 2005. Atmospheric Pressure Chemical Vapor Deposition of Crystalline Monoclinic  $\text{WO}_3$  and  $\text{WO}_{3-x}$  Thin Films from Reaction of  $\text{WCl}_6$  with O-Containing Solvents and Their Photochromic and Electrochromic Properties. *Chem. mater.* 17 (6) 1583-1590.  
 [10] Jin-Ho Choy, Kim Y, Whan Kim B, Park N, Campet G, Grenier J, 2000. New Solution Route to Electrochromic Poly(acrylic acid)/ $\text{WO}_3$  Hybrid Film, *Chem. Mater.* 12 2950-2956.  
 [11] Deepa M, Srivastava A. K, Agnihotry S. A, 2006. Photoelectrochemical Properties of  $\text{WO}_3$  Thin Films Prepared by Electrodeposition, *Acta. Mater.* 54 4583-4595.  
 [12] Jinmin Wang, Khoo E, See Lee P, Ma J, 2008. Synthesis, Assembly, and Electrochromic Properties of Uniform Crystalline  $\text{WO}_3$  Nanorods, *J. Phys. Chem. C* 112 14306-14312.  
 [13] ScZancoski J. C, Cavalcante L. S, Joya M. R, Varela J. A, Pizani P. S, Longo E, 2008.  $\text{SrMoO}_4$  powders processed in microwave-hydrothermal: Synthesis, characterization and optical properties, *Journal of Alloys and Compounds* 140 632-637.  
 [14] WeiWang et.al, Synthesis of well-defined hierarchical porous  $\text{La}_2\text{Zr}_2\text{O}_7$  monoliths via non-alkoxide sol-gel process accompanied by phase separation, *Journal Microporous and Mesoporous Materials*, 221, 32-39.  
 [15] Abraham Wolcott, Kuykendall T. R, Chen W, Shaowei C, Zhang J. Z, 2006. Synthesis and Characterization of Ultrathin  $\text{WO}_3$  Nanodisks Utilizing Long-Chain Poly(ethylene glycol), *J. Phys. Chem. B* 110 25288-25296.  
 [16] Fusongjiang, Zheng T, Yang Y, 2008. Preparation and electrochromic properties of tungsten oxide and iridium oxide porous films, *Journal of Non-Crystalline Solids* 354 1290-1293.  
 [17] Deepa M, Srivastava A. K, Sharma S. N, Govind, Shivaprasad S. M, 2008. Microstructural and electrochromic properties of tungsten oxide thin films produced by surfactant mediated electrodeposition, *Applied Surface Science* 254 2342-2352.



- [18] Deepa M, Singh D. P, Shivaprasad S. M, Agnihotry S. A, 2007. A comparison of electrochromic properties of sol-gel derived amorphous and nanocrystalline tungsten oxide films, *Current Applied Physics* 7 220-229.
- [19] Jiun-ChanYang Dutta P. K, 2009. Solution-based synthesis of efficient WO<sub>3</sub> sensing electrodes for high temperature potentiometric NO<sub>x</sub> sensors, *Sensors and Actuators B* 136 523-529.
- [20] Deepa M, Srivastava A. K, Agnihotry S. A, 2006. Influence of annealing on electrochromic performance of template assisted, electrochemically grown, nano-structured assembly of tungsten oxide, *Acta Materialia* 54 4583-4595.
- [21] Deepa M, Srivastava A. K, Agnihotry S. A, Kar M, 2006. A case study of optical properties and structure of sol-gel derived nanocrystalline electrochromic WO<sub>3</sub> films, *Electro chimica Acta*, 51 1974-1989.
- [22] Deepa M, Sharma R, Basu A, Agnihotry S. A, 2005. Effect of oxalic acid dihydrate on optical and electrochemical properties of sol-gel derived amorphous electrochromic WO<sub>3</sub>, *Electro chimica Acta* 50 3545-3555.
- [23] Dattatray J, Late J, Ranjit. Chandra Sekhar Rout K, Mahendra A, More S, Dilip, Joag S, 2010. Low threshold field electron emission from solvothermally synthesized WO<sub>2.72</sub> nanowires, *Apply. Phy A*, 98 751-756.
- [24] Mauro E, Teresa A, Jordi A, Raúl D, SICILIANO Pietro, Mornate Joan R, 2009. The Chloroalkoxide Route to Transition Metal Oxides. Synthesis of V<sub>2</sub>O<sub>5</sub> Thin Films and Powders from a Vanadium Chloromethoxide, *Chemistry of Materials*, 21 5215-5221.
- [25] Escobedo Morales A, S´anchez Mora E, Pal U, 2006. Use of diffuse reflectance spectroscopy for optical characterization of un-supported nanostructures, *Rev. Mex. Fis.* 53 18-22.